

AKAP121 downregulation impairs protective cAMP signals, promotes mitochondrial dysfunction, and increases oxidative stress

Cinzia Perrino^{1,2*}, Antonio Feliciello^{3*}, Gabriele G. Schiattarella¹, Giovanni Esposito¹, Rosalia Guerriero¹, Laura Zaccaro⁴, Annarita Del Gatto⁴, Michele Saviano⁴, Corrado Garbi³, Rosa Carangi², Emilio Di Lorenzo¹, Giuseppe Donato⁵, Ciro Indolfi⁵, Vittorio Enrico Avvedimento³, and Massimo Chiariello¹

¹Division of Cardiology, Department of Clinical Medicine, Cardiovascular and Immunological Sciences, Federico II University, Via Pansini 5, Naples 80131, Italy; ²Istituto Neurologico Mediterraneo, Pozzilli (IS), Italy; ³Department of Molecular and Cellular Pathology, Federico II University, Via Pansini 5, Naples 80131, Italy; ⁴Istituto di Biostrutture e Bioimmagini (CNR), Naples, Italy; and ⁵Magna Graecia University, Catanzaro, Italy

Received 3 December 2009; revised 5 May 2010; accepted 26 May 2010; online publish-ahead-of-print 28 May 2010

Time for primary review: 25 days

Aims The aim of the present study was to determine the function and the role of the scaffold protein AKAP121, tethering cAMP dependent protein kinase A to the outer wall of mitochondria, in neonatal ventricular myocytes and the heart.

Methods and results Competitive peptides displacing AKAP121 from mitochondria in the tissue and in the cells were used to investigate the role of AKAP121 in mitochondrial function, reactive oxygen species (ROS) generation, and cell survival. Displacement of AKAP121 from mitochondria by synthetic peptides triggers the death program in cardiomyocytes. Under pathological conditions *in vivo*, in a rat model of cardiac hypertrophy induced by ascending aorta banding, the levels of AKAP121 are significantly down-regulated. Disappearance of AKAP121 is associated with mitochondrial dysfunction, high oxidative stress, and apoptosis. *In vivo* delocalization of AKAP121 by competitive peptides replicates some of the molecular signatures induced by pressure overload: mitochondrial dysfunction, increased mitochondrial ROS, and apoptosis.

Conclusion These data suggest that AKAP121 regulates the response to stress in cardiomyocytes, and therefore AKAP121 down-regulation might represent an important event contributing to the development of cardiac dysfunction.

Keywords Mitochondria • Heart failure • Protein kinase A • Oxygen radicals

1. Introduction

β -Adrenergic receptors (β AR) are important regulators of cardiac function, increasing the intracellular levels of cAMP and activating the cAMP-dependent protein kinase A (PKA).^{1,2} Abnormalities in β AR signalling are hallmarks of cardiac hypertrophy and heart failure, linked to the development of cardiac dysfunction.^{1,2} Whereas most studies have focused on alterations at the level of the receptor,^{1,2} evidence for defects distal to the β AR/adenylyl cyclase complex is also accumulating.^{3,4}

A large group of proteins that anchor PKA to membranes and cellular organelles (A Kinase Anchor Proteins, AKAPs) have been recently recognized as important players in the propagation of

cAMP signals.^{5,6} Acting as scaffolds, AKAPs recruit signalling molecules and present them to downstream targets to achieve efficient spatial and temporal control of their phosphorylation state. Recent reports have pointed at AKAPs as important players in the development of cardiomyocyte hypertrophy.^{7,8} Muscle AKAP (mAKAP) and AKAP-lbc (lymphoid blast crisis oncogene) have been shown to potentiate *in vitro* cardiomyocytes hypertrophy,^{7,8} while AKAP79 has been shown to reduce cardiac hypertrophy induced by pressure overload or chronic catecholamine stimulation.⁹

Mitochondria are important generators of energy and a major site of reactive oxygen species (ROS) production, which may contribute to the development of cardiac dysfunction. cAMP signals are carried to mitochondria by a set of mitochondrial AKAPs. AKAP121 (also

called D-AKAP1) and its smaller variant AKAP84 are prototypic mitochondrial PKA anchor proteins that arise from a single gene by alternative mRNA splicing.¹⁰ Accumulation of AKAP84/121 and their cognate mRNA are positively regulated by cAMP/PKA pathway.¹¹ AKAP121 has been recently identified as an essential regulator of mitochondrial respiration,¹⁰ nucleating a multivalent signalling complex that includes PKA, tyrosine phosphatase (PTPD1), and src (proto-oncogene from avian sarcoma) on the outer wall of mitochondria.^{12,13} AKAP84/121 are both widely expressed in different tissues and cell types, including ventricular tissue.¹⁴ It has been recently shown that AKAP121 negatively regulates cardiomyocytes hypertrophy *in vitro*,¹⁵ however its *in vivo* function and regulation are currently unknown.

In this study, we investigated the role of mitochondrial AKAPs in the modulation of mitochondrial function, ROS production, and cell survival *in vitro* and *in vivo*. Displacement of AKAP121 from mitochondria by competitive peptides increased ROS levels and promoted cell death in muscle cells and the heart. In response to pressure overload, AKAP121 downregulation was associated with mitochondrial stress, increased ROS production, and cell death, suggesting that dampened mitochondrial cAMP signalling might contribute to the development of cardiac dysfunction.

2. Methods

An expanded material and methods section describing cell culture studies, immunofluorescence analysis, RNA extraction, Northern Blotting, total protein extraction, sub-cellular fractionation, immunoblot analysis, antibodies, real-time PCR, and mini-osmotic pump implantation is given in the Supplementary material online.

2.1 Animal studies

All experiments involving animals were conform to the Guide for the Care and Use of Laboratory Animals published by the US National Institutes of Health (NIH Publication No. 85-23, revised 1996) and were approved by the animal welfare regulation of University Federico II of Naples, Italy. Animals were maintained under identical conditions of temperature ($21 \pm 1^\circ\text{C}$), humidity ($60 \pm 5\%$), and light/dark cycle, and had free access to normal rodent chow.

2.2 Rat model of pressure overload

Male adult Wistar rats (age 9–11 weeks; 250–300 g; $n = 71$) were anaesthetized with an intramuscular injection of ketamine 100 mg/kg and xylazine 5 mg/Kg (Sigma-Aldrich). Left ventricular hypertrophy (LVH) was induced by ascending aortic constriction using a tantalum clip (Weck Inc.) of 0.58 mm internal diameter placed on the ascending aorta via a thoracic incision as previously described.¹⁶ Animals were sacrificed 3 (LVH3, $n = 16$), 6 (LVH6, $n = 15$), and 12 (LVH12, $n = 20$) days after surgery to perform molecular or histological analyses. Additional age-matched animals underwent a left thoracotomy without placement of the clip; in those animals, the hearts were removed 12 days after surgery (SHAM, $n = 20$). Cardiac function was monitored by transthoracic echocardiography using an ultrasound apparatus HP SONOS 5500 equipped with a 7.5 MHz phased-array transducer before the surgery and after 3, 6, and 12 days. At sacrifice, rats were anaesthetized as described above, and after body weight (BW) calculation, invasive LV end-diastolic (LVEDP) and end-systolic pressures (LVESP) were measured with a 1.4-Fr (0.46 mm) high-fidelity conductance catheter (Millar Instruments, TX, USA) inserted into the right carotid and advanced retrograde into the left ventricle (LV). After a brief period of stabilization, LV pressure was recorded. The hearts were then removed and cardiac chambers were

dissected to assess left ventricular (LV) and right ventricular weights. Each LV was sectioned in two segments: a proximal segment including the base that was fixed in 4% formaldehyde for histological studies, and a distal segment including the apex that was flash-frozen in liquid nitrogen for the biochemical analysis. RNA and protein analyses were performed in the same hearts. After termination, tibial length (T) was also determined.

2.3 Morphological studies

Rat and mouse LV specimens were fixed in 4% formaldehyde and embedded in paraffin. After de-paraffinization and re-hydration, 4 μm thick sections were prepared, mounted on glass slides, and stained with haematoxylin–eosin. The DNA nicks were determined with the use of an *in situ* Apoptosis Detection kit or ApopTag Fluorescein Direct *in Situ* Apoptosis Detection kit (Chemicon) according to manufacturer's instructions. For rat specimens, TUNEL staining was visualized with 3,3'-diaminobenzidine (DAB, Vector), which stained the nuclei with DNA damage brown. Cardiac sections were then counterstained with methyl green (Carlo Erba). For mouse LV specimens, TUNEL staining was visualized by specific green fluorescence and nuclei by 4'-6-diamidino-2-phenylindole (DAPI). The number of TUNEL-positive cardiomyocyte nuclei was counted, and data were normalized per total nuclei identified by methyl green (rat hearts) or DAPI staining (mouse hearts) in the same sections ($n = 3-4$ animals/group).

ROS production was assessed by dihydroethidium (DHE) conversion to red fluorescent ethidium. Five micrometre thick LV sections were dewaxed, rehydrated, incubated at room temperature with DHE (Sigma-Aldrich; 10 $\mu\text{mol/L}$) in Krebs buffer for 30 min, and protected from light. Images were acquired in the first 30 s of light exposure under an Axiophot-2 fluorescence microscope (ZEISS) and analysed using a digital camera system coupled to an imaging software (Spot, Diagnostic Instrument). In order to quantify DHE staining, fluorescence intensity was measured in 6 fields/section, averaged, and expressed as arbitrary units ($n = 3-4$ animals/group).

Mitox Red (Molecular Probes) was used as an indicator to assess the generation of mitochondrial superoxide. Ten microgram of Mitox Red in 200 μL phosphate-buffered saline was injected into the tail vein of each group of mice. Animals were sacrificed 90 min later, the hearts were rapidly removed, LV dissected, and fixed overnight in 4% paraformaldehyde, included in optimum cutting temperature compound (OCT, Miles Pharmaceuticals), and snap frozen in liquid nitrogen. Ten micrometre LV sections were cut using a cryostat.

Immunohistochemistry with antinitrotyrosine antibodies recognizes the reaction products of oxygen-free radicals with nitric oxide, such as peroxynitrite, on tyrosine residues of proteins. For the measurement of peroxynitrite, rat LV sections contiguous to those treated with DHE were blocked at room temperature with 3% normal goat serum and 0.1% Triton-X in TBS for 1 h and then incubated with anti-nitrotyrosine antibodies (rabbit, 5 $\mu\text{g/mL}$ Upstate biotechnology) overnight at 4°C . The immunoreactivity was visualized with the use of Vectastain ABC kit (Vector). All the sections were examined with a microscope (Leitz, DIAPLAN) and images were acquired with a digital camera (Digital JVC, TK-C1380). The staining of bound antibodies was visualized with DAB (Vector) and quantified as percentage of stained area over total ventricular area from digital photomicrograph images ($n = 3-4$ animals/group, 6 fields/section).

In order to perform ultrastructural analysis by electron microscopy, rat left ventricular specimens were fixed in 3% glutaraldehyde/0.1 M phosphate buffer and processed (post-fixation and dehydration) for embedding in Epon-Araldite. Ultra-thin sections, stained with uranyl acetate and lead citrate, were studied with a Zeiss EM 900 electron microscope.

2.4 Peptide synthesis and characterization

P_{mit} peptides encompass the 15–21 region of AKAP121 mitochondrial targeting domain.¹⁷ In order to increase water solubility, the peptide

was modified introducing two lysine residues at both termini. In addition, the peptide was acetylated and amidated at N- and C-terminal to reduce the helical dipole charge. FP_{mit} is an analog of AKAP_{wt} peptide as previously reported,¹⁸ encompassing the 10–30 regions of AKAP121 mitochondrial targeting domain¹⁷ and is functionalized at N-terminus with fluorescein. P_{cn} is a peptide used as control sequence; FP_{cn} is functionalized at the N-terminus with fluorescein.

All peptides were manually synthesized on solid phase by Fmoc chemistry (9-fluorenylmethoxycarbonyl) using all standard amino acids. The syntheses of P_{mit} (Ac-KKGLMLALLGKK-NH₂) and FP_{mit} (Fluo-XXXPLALPGMLALLGWWWFFSRKXX-NH₂) were carried out with Fmoc-PAL-PEG-PS resin. P_{cn} (H-RNPHKGPAT-OH) was synthesized using Rink Amide MBHA resin. The Fmoc deprotection step was performed with piperidine in DMF (N,N dimethylformamide). All amino acids were coupled according to the HBTU (O-Benzotriazole-N,N,N',N'-tetramethyl-uronium-hexafluoro-phosphate)/HOBt(N-Hydroxybenzotriazole)/DIPEA (N, N diisopropylethylamine) method. Each coupling was followed by a capping step performed with acetic anhydride/DIPEA/HOBt/DMF. Before the final Fmoc deprotection, the N-terminus of P_{mit} was acetylated by acetic anhydride/DIPEA/HOBt in DMF. In contrast, the N-terminus of FP_{mit} was labelled using 6-[Fluorescein-5(6)-carboxamido]hexanoic acid/HATU O-(7-azabenzotriazol-1-yl)-N,N,N',N'-tetramethyluronium/DIPEA in DMF. Cleavage of peptides from the resins was achieved by treatment with a mixture of TFA (trifluoroacetic acid) /H₂O/EDT (ethanedithiol) /TIS (triisopropylsilane). Then, all peptides were precipitated by cold ethyl ether, dissolved in acetonitrile and water, and lyophilized. The crude products were purified by preparative RP-HPLC on C₁₈ column and a linear gradient of H₂O-0.1% TFA (A)/CH₃CN-0.1%TFA (B) from 20 to 80% of B in 20 min at flow rate of 20 mL/min. Peptide purity and identity were assessed by LC-MS.

For all *in vitro* experiments, cultured cells [smooth muscle cells (SMCs) or neonatal ventricular myocytes (NVMs)] were perfused with P_{mit} /FP_{mit} or P_{cn} /FP_{cn} peptides for 24 h at 37°C and 5% CO₂. Changes in mitochondrial aconitase activity were detected using a BIOXYTECH[®] Aconitase-340TM kit (OxisResearch) in mitochondrial fractions obtained from cultured cells and left ventricular samples according to the manufacturer's instructions. Aconitase activity was expressed as microU of *cis*-aconitase converted per minute per milligram of mitochondrial protein.

In order to quantify total and mitochondrial ATP levels, cultured SMCs treated with P_{mit} or P_{cn} peptides were incubated in the presence or absence of Rotenone 5 μM (Sigma-Aldrich) for 45 min. Assays were performed using the ATP luminescence assay kit HS II (Roche) according to the manufacturer's instructions, using 5000 cells/sample. Light emission was recorded in a single measure of 2 s using a Lumat LB 9507 luminometer (Berthold Technologies). The emission recorded from samples treated with rotenone was defined as baseline luminescence corresponding to a non-mitochondrial source of ATP. The difference between emissions recorded from untreated samples (total ATP) and Rotenone-treated cells was defined as the mitochondrial source of ATP.

In order to test the effects of P_{mit} or P_{cn} peptides on cell survival, cultured SMCs and NVMs were stained with propidium iodide (PI) according to the manufacturer's instructions (Sigma-Aldrich). Cultured SMCs were treated with P_{mit} or P_{cn} peptides, harvested by trypsinization, and combined with floating cells. Cells were then stained with PI, and DNA content was analysed by flow cytometry. All flow cytometry analyses were performed on a flow cytometer equipped with a 25 mW argon ion laser for excitation at 488 nm (FACSCalibur, Becton & Dickinson) and the data were analysed with the Cell Quest software (Becton & Dickinson). All analyses were repeated three to four times with different preparations of cells. Gating was set to exclude debris and cellular aggregates, and 10 000 or more events were counted for each analysis. NVMs were plated on glass slides, incubated with FP_{mit} or FP_{cn} peptides, and then stained with PI. Slides were analysed with a Nikon microscope (Eclipse 2000) or with a Zeiss 510 confocal laser scanning microscope.

Intracellular ROS were detected in cultured SMCs by assessing oxidation of 2', 7'-dichlorofluorescein-diacetate (DCFH-DA) by flow cytometry. A 10 mM stock solution of DCFH-DA was prepared in ethanol on a daily basis. SMC cultures were treated with DCFH-DA (10 μM) for 30 min at room temperature in the dark, and then analysed by flow cytometry as described above.

Mitochondrial membrane potential ($\Delta\psi_m$) was assessed by flow cytometry using tetramethylrhodamine ethyl ester (TMRE, Molecular Probes), a non-toxic monovalent cation that reversibly accumulates in the mitochondrial lipid environment according to membrane potential with a Nernstian distribution. After specific treatment, cultured SMCs were resuspended in their complete media and incubated with 50 nM of TMRE for 20 min in the dark at 37°C. At the end of incubation, cells were re-suspended in the flow analysis buffer (PBS 1X), and kept on ice until analysed.

In SMC and NVM cultures, superoxide production by mitochondria was visualized by Mitosox Red mitochondrial superoxide indicator (Molecular Probes) according to the manufacturer's instructions. Briefly, cultured NVMs or SMCs were perfused with P_{mit} or P_{cn} peptides as describe above, incubated with the Mitosox reagent for 10 min, and then visualized with a Zeiss 510 confocal laser scanning microscope.

2.5 *In vivo* peptide administration

In order to test the *in vivo* effects of the peptides, 300 μg of FP_{mit}, FP_{cn}, P_{mit}, and P_{cn} peptides were dissolved in 300 μL of saline at a final concentration of 1 μg/μL. Wild-type C57BL/6 mouse (9-week-old; 25–30 g) underwent daily intraperitoneal injections of 100 μL of saline (vehicle) or specific peptides. After 3 days of treatment, the animals were anaesthetized as described above and sacrificed. Cardiac chambers were dissected and weighed. The left ventricle and samples from liver and kidney were snap-frozen in liquid nitrogen or fixed in buffered formalin for further analyses. For LV samples, non-specific fluorescence was prevented incubating free-floating tissue sections in a solution of sodium borohydride (NaBH₄; 0.1–2.0% in PBS 1X; Sigma-Aldrich) for 30 min.¹⁹

2.6 Statistical analysis

The data are presented as mean ± SE. Differences between experimental groups were evaluated for statistical significance using Student's *t*-test for unpaired data or one-way analysis of variance with Bonferroni correction. For all analyses, a minimum value of *P* < 0.05 was considered significant, when present, a *P*-value < 0.01 was specified. All statistical analyses were performed using GraphPad Prism 4 (GraphPad Software version 4.0).

3. Results

3.1 AKAP121 levels are regulated by cAMP in smooth muscle cells and cardiomyocytes

Under various pathological conditions, both the heart and vessels undergo morphological alterations that can eventually lead to heart failure. Thus, understanding the mechanisms that control growth and survival in vascular SMCs and NVMs is an important step to develop novel therapeutic interventions for cardiovascular diseases. Although both SMCs and NVMs are muscle cell types, they vary in their mechanisms of contraction, growth, and differentiation. For these reasons, in this study, both rat vascular SMCs and NVMs were used.

AKAP121 is abundantly expressed in both rat NVMs and SMCs (Figure 1A). To analyse the intracellular location of AKAP121, NVM and SMC cultures were stained with a specific anti-AKAP121 antibody and mitotracker, a dye that selectively accumulates in vital mitochondria. Both in NVM and SMC cultures, AKAP121 staining was specific

and mostly localized to the perinuclear region, where it largely overlapped with mitotracker (Figure 1B).

In cultured SMCs, stimulation for 24 h with cAMP increased the levels of AKAP121; pre-treatment with a specific PKA inhibitor (H89) abrogated this effect (Figure 1C). Similarly, NVM cultures were treated with the β -agonist isoproterenol (10 μ M, ISO) displayed a significant induction of AKAP121 levels after 12 h incubation (Figure 1D, upper panel). Under the same conditions, NVMs accumulated phospho-CREB_{Ser133} (Figure 1D, middle panel), suggesting that AKAP121 levels are regulated by cAMP *in vitro* in muscle cells.

3.2 AKAP121 mitochondrial delocalization impairs mitochondrial function and lowers the tolerance to oxidative stress of smooth muscle cells

To investigate the role of AKAP121 in mitochondrial function, ROS generation, and cell survival, synthetic peptides spanning the mitochondrial targeting domain of AKAP121 (P_{mit})²⁰ were designed to competitively displace endogenous AKAP121 from mitochondria. Control peptides (P_{cn}) were used to validate the specificity of peptides P_{mit} . P_{mit} peptides conjugated with fluorescein (FP_{mit}) selectively

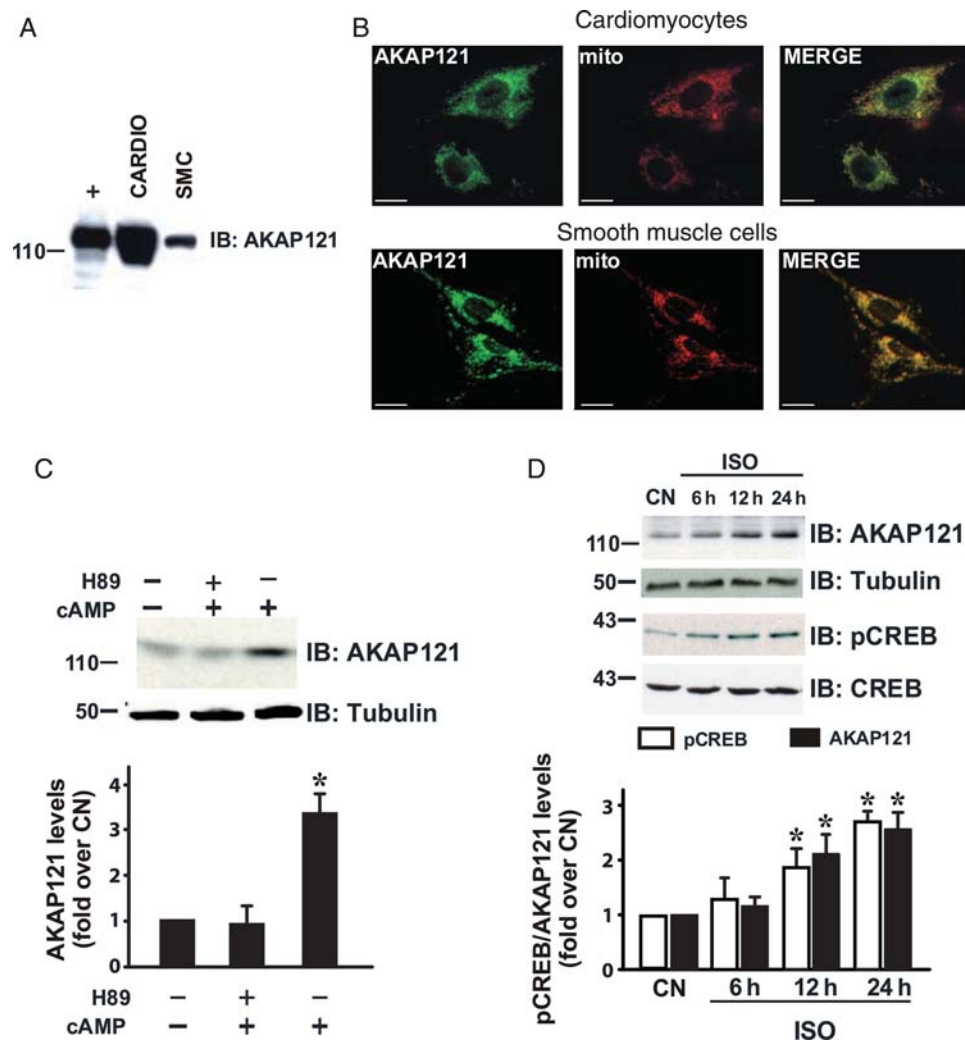


Figure 1 Expression and regulation of AKAP121 in cardiomyocytes and smooth muscle cells. (A) AKAP121 levels in total protein lysates (100 μ g) of neonatal ventricular myocytes (NVMs) and smooth muscle cells (SMCs) separated in 8% SDS/polyacrilamide gels. Molecular weight markers (kDa) are reported on the left. Total cell lysates from HEK 293 cells transfected with AKAP121 cDNA were used as positive controls (+). (B) Immunofluorescence analysis of cultured NVMs and SMCs stained with anti-AKAP121 antibodies and visualized with fluorescein-tagged goat antirabbit IgG (AKAP121, green). Mitochondria were visualized in the same cells by staining with mitotracker-red (mito). Scale bar = 10 μ m. (C) Representative immunoblot and densitometric analysis of three independent experiments to evaluate AKAP121 protein levels in SMCs incubated with CPT-cAMP (250 μ M) for 24 h with or without H89 25 μ M (CN = control; * P < 0.01 for cAMP vs. CN or cAMP/H89). Tubulin protein levels did not significantly change among the samples. In these experiments, 40 μ g of proteins were loaded in each lane. (D) Representative immunoblots and densitometric analysis of three independent experiments to evaluate AKAP121, pCREB, or CREB protein levels in NVMs stimulated with Isoproterenol (ISO) 10 μ M at different time points (* P < 0.05 for 12 h ISO and 24 h ISO vs. CN or 6 h ISO). Tubulin and total CREB levels did not significantly change.

accumulated in the perinuclear region of SMCs (see Supplementary material online, *Figure S1A*). In cultured cells perfused with P_{mit} peptides, endogenous AKAP121 was displaced from mitochondria, and this effect was specific, since control peptides (P_{cn}) did not alter mitochondrial localization of AKAP121 (Supplementary material online, *Figure S1B*). The competitive displacement of endogenous AKAP121 from mitochondria by P_{mit} peptides was also confirmed by immunoblot analysis of mitochondrial fractions of SMCs (Supplementary material online, *Figure S1C*).

Compared with control cells (untreated or P_{cn} -treated), P_{mit} peptides significantly inhibited mitochondrial aconitase activity (Supplementary material online, *Figure S1D*). Furthermore, P_{mit} peptides significantly reduced the oxidative ATP synthesis in SMC cultures (Supplementary material online, *Figure S1E*) and mitochondrial membrane potential ($\Delta\psi_m$) assessed by TMRE (TMRE mean fluorescence: $P_{cn} = 9.5 \pm 0.3$, $P_{mit} = 7.5 \pm 0.6$, -21% reduction compared with P_{cn} , $P < 0.05$), suggesting that AKAP121 de-localization promotes mitochondrial dysfunction.

To test whether P_{mit} peptides might affect ROS production, the oxidation of 2', 7'-dichlorofluorescein-diacetate (DCFH-DA) was measured by flow cytometry in P_{mit} -treated SMCs cultures. After 24 h incubation, P_{mit} peptides induced a significant increase in the oxidation of DCFH (Supplementary material online, *Figure S1F*). Since DCFH can be oxidized by various ROS, peroxynitrite, intracellular oxidases, and peroxidases, we next directly visualized mitochondrial generation of superoxide as red fluorescence by Mitosox oxidation in SMC cultures. As shown in Supplementary material online, *Figure*

S1G, P_{mit} peptides induced a marked increase in Mitosox oxidation compared with P_{cn} peptides.

In order to test whether P_{mit} peptides affected cell viability under basal and stress conditions, SMC cultures were perfused with control medium (–), P_{mit} , or P_{cn} peptides for 24 h, and subsequently treated with H_2O_2 (50 μM) for 2 min. While under basal conditions, P_{mit} peptides did not affect SMCs viability, they enhanced robustly cell death induced by oxidative stress (Supplementary material online, *Figure S1G*). These data indicate that AKAP121 controls mitochondrial activity and resistance to oxidative stress in SMCs.

3.3 AKAP121 mitochondrial delocalization increases oxidative stress and directly promotes cell death in cardiomyocytes

In order to determine the effects of AKAP121 mitochondrial delocalization in cardiac cells, NVM cultures were perfused with P_{mit} or P_{cn} peptides, and AKAP121 subcellular localization was tested by immunoblotting. Consistent with our results in SMC cultures, AKAP121 mitochondrial levels were significantly reduced in P_{mit} -treated NVM cultures (*Figure 2A*). Next, to test whether AKAP121 displacement would affect mitochondria-generated superoxide, NVM cultures were perfused with P_{mit} peptides and Mitosox oxidation was analysed. P_{mit} -treated NVM cultures exhibited a marked increase in mitochondrial ROS compared with P_{cn} -treated cell cultures (*Figure 2B*). Finally, to test the effects of AKAP121 delocalization on survival, PI staining was performed in NVMs treated with FP_{mit} or FP_{cn} peptides.

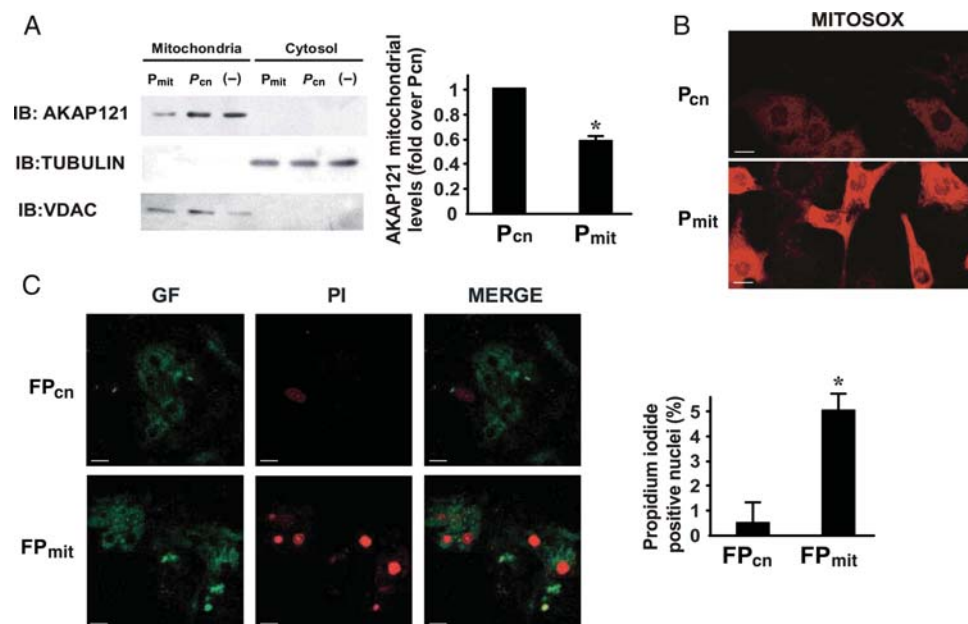


Figure 2 Effects of AKAP121 delocalizing peptides on mitochondrial ROS generation and cell survival in cardiomyocytes. (A, left panels) Representative immunoblots of AKAP121, tubulin, and VDAC protein levels in mitochondrial and cytosolic fractions of NVMs treated with P_{cn} or P_{mit} peptides. (Right panel) Densitometric analysis of three independent experiments on AKAP121 levels in mitochondrial fractions ($*P < 0.01$ vs. P_{cn}). (B) Representative confocal microscopy images illustrating mitochondrial ROS production in cultured NVMs incubated with P_{cn} or P_{mit} peptides by Mitosox staining. Scale bar = 10 μm . (C, left panels) Representative confocal microscopy images illustrating red propidium iodide (PI) staining in cultured NVMs incubated with P_{cn} or P_{mit} peptides conjugated with fluorescein (FP_{cn} , FP_{mit}). Scale bar = 10 μm . (Right panel) Cumulative data of the PI staining of three independent experiments ($*P < 0.01$ vs. FP_{cn}). In each experiment, 6–10 fields were acquired, analysed, and averaged.

Interestingly, FP_{mit} peptides induced marked positivity to PI staining in unstressed NVMs (Figure 2C), suggesting that these cells are more sensitive and vulnerable to AKAP121 mitochondrial delocalization and increased ROS generation.

3.4 Impaired transmission of cAMP signals to nuclei and mitochondria in cardiac hypertrophy induced by pressure overload

Since AKAP121 levels were regulated by cAMP in muscle cells, we next assessed AKAP121 regulation in a rat model of left ventricular hypertrophy (LVH) induced by pressure overload.¹⁶ As expected, this model rapidly caused cardiac hypertrophy in rats, as shown by the increase in the left ventricle weight after 3 days of pressure overload, even when normalized to BW or tibial length (Table 1). After 12 days of pressure overload (LVH12), diastolic and systolic dysfunction could be detected, as shown by increased LVEDP pressure and reduced LV% fractional shortening, respectively (Table 1). At this time point (LVH12), histological analysis showed interstitial fibrosis (Figure 3A) and foetal genes of atrial natriuretic peptide (ANP) and brain natriuretic peptide (BNP) were significantly re-activated (Table 1). Furthermore, β -adrenergic receptor kinase 1 (β ARK1) levels were robustly up-regulated (Table 1). Activation of de-sensitization mechanisms reduced the transmission of cAMP signals to the nuclei, since phosphorylation of the nuclear transcriptional factor CREB (cAMP response element-binding protein) at

Ser₁₃₃ was significantly reduced in LVH hearts (Figure 3B). Interestingly, AKAP121 mRNA and protein levels were significantly reduced in response to pressure overload (Figure 3C and D). Under these conditions, SHAM and LVH animals displayed similar levels of total PKA regulatory RII subunit (Figure 3D).

3.5 Altered mitochondrial structure and increased oxidative stress in pressure-overloaded hearts

To test whether AKAP121 downregulation in response to pressure overload was associated with mitochondrial abnormalities, electron microscopy studies on cardiac sections from SHAM and LVH12 hearts were performed. Compared with SHAM, LVH12 hearts displayed remarkable ultrastructural signs of mitochondrial stress, including matrix swelling and cristae disarray (Figure 4A). These structural abnormalities were associated with the evidence of mitochondrial dysfunction, such as reduced mitochondrial aconitase activity (Figure 4B).

To determine whether mitochondrial dysfunction in cardiac hypertrophy would translate into increased ROS generation, the conversion of DHE to red fluorescent ethidium, and the amount of peroxynitrite on tyrosine residues of proteins were analysed and measured in cardiac sections from SHAM and LVH12. In response to pressure overload, DHE and nitro-tyrosine staining were both significantly increased compared with the SHAM condition (Figure 4C and D). In the same hearts, an increased TUNEL staining could also be

Table 1 Left ventricular hypertrophy induced by ascending aortic banding in rats

	SHAM	LVH3	LVH6	LVH12
<i>Morphometry</i>	(n = 15)	(n = 16)	(n = 15)	(n = 14)
BW (g)	265 ± 6	271 ± 5	275 ± 4	281 ± 7
T (mm)	50.1 ± 1.1	50.9 ± 0.8	51.8 ± 1	52.1 ± 1.1
H (g)	1.0 ± 0.03	1.3 ± 0.05*	1.3 ± 0.03*	1.5 ± 0.04*
LVW (g)	0.6 ± 0.02	0.9 ± 0.02*	1.0 ± 0.04*	1.2 ± 0.02*
RV (g)	0.36 ± 0.03	0.38 ± 0.04	0.39 ± 0.03	0.4 ± 0.04
LVW/BW (mg/g)	2.19 ± 0.4	3.06 ± 0.3*	3.60 ± 0.3*	4.27 ± 0.5*
LVW/T (mg/mm)	11.6 ± 0.7	16.3 ± 0.6*	19.1 ± 0.5*	23.1 ± 0.8*
LVEDP (mmHg)	5.5 ± 0.5	5.8 ± 0.6	6.1 ± 0.5	10.4 ± 0.8†
LVESP (mmHg)	105 ± 6	196 ± 5*	201 ± 6*	189 ± 8*
<i>Echocardiography</i>	(n = 6)			(n = 7)
LVEDD (mm)	6.4 ± 0.37			6.3 ± 0.26
LVESD (mm)	2.7 ± 0.16			3.4 ± 0.14‡
FS (%)	55.4 ± 3.3			48.5 ± 1.9‡
IVSd (mm)	1.5 ± 0.09			1.8 ± 0.07‡
PWd (mm)	1.4 ± 0.08			1.9 ± 0.08‡
LVM (g)	0.56 ± 0.33			0.69 ± 0.28‡
HR (bpm)	288 ± 76			270 ± 90.39
<i>Gene/protein expression</i>	(n = 3)			(n = 4)
ANP mRNA levels (fold over SHAM)	1.0			3.9 ± 0.23*
BNP mRNA levels (fold over SHAM)	1.0			3.8 ± 0.21*
β ARK1 protein levels (fold over SHAM)	1.0			3.5 ± 0.53*

SHAM, sham-operated control animals; LVH3, aortic banded animals, 3 days after surgery; LVH6, aortic banded animals, 6 days after surgery; LVH12, aortic banded animals, 12 days after surgery; BW, body weight; T, tibial length; H, heart weight; LVW, left ventricular weight; RV, right ventricular weight; LVEDP, LV end-diastolic pressure; LVESP, LV end-systolic pressure; LVEDD, left ventricular end-diastolic diameter; LVESD, left ventricular end-systolic diameter; FS, fractional shortening; IVSd, end-diastolic interventricular septum; PWd, end-diastolic posterior wall; LVM, left ventricle mass; HR, heart rate; ANP, atrial natriuretic peptide; BNP, brain natriuretic peptide; β ARK1, β -adrenergic receptor kinase 1 (*P < 0.01 vs. SHAM, †P < 0.05 vs. SHAM, LVH3, and LVH6, ‡P < 0.05 vs. SHAM). In SHAM rats, the hearts were removed 12 days after surgery.

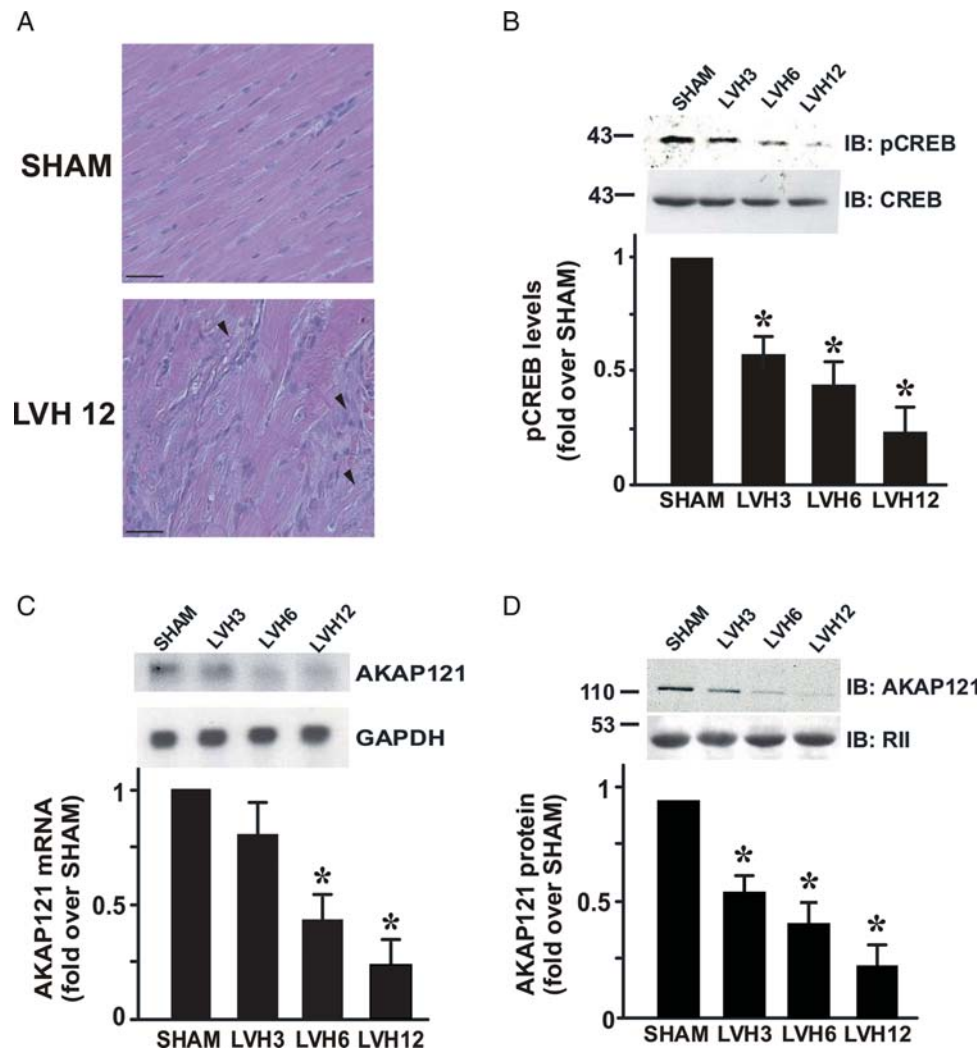


Figure 3 Regulation of AKAP121 levels in the rat model of pressure overload. (A) Representative haematoxylin–eosin staining in cardiac sections from SHAM and LVH12 rat hearts. Arrow heads indicate fibrosis areas. Scale bar = 50 μ m. (B) Representative immunoblots and densitometric analysis of four independent experiments to evaluate pCREB and CREB levels in SHAM and LVH hearts (for pCREB, $*P < 0.05$ vs. SHAM). In the same samples, total CREB protein levels did not significantly change among the different groups. (C) AKAP121 mRNA levels analysed by northern blotting in hearts from SHAM and LVH rats ($n = 4$ hearts/group; $*P < 0.05$ vs. SHAM or LVH3). In the same samples, GAPDH mRNA levels did not significantly change among the different groups. (D) Representative immunoblots and densitometric analysis of four independent experiments to evaluate AKAP121 protein levels in SHAM and LVH hearts ($*P < 0.05$ vs. SHAM or LVH3). In the same samples, RII protein levels did not significantly change among the different groups.

found (Figure 4E). These findings suggest that AKAP121 downregulation in pressure overload-induced cardiac hypertrophy is associated with mitochondrial dysfunction, increased ROS generation, and cell death.

3.6 AKAP121 mitochondrial delocalization increases oxidative stress and promotes cell death in the mouse heart

To evaluate the *in vivo* effects of AKAP121 competitive displacement, wild-type C57BL/6 mice were treated with FP_{mit}, FP_{cn} peptides, or vehicle (saline) for 3 days by intra-peritoneal injections. Cardiac localization of administered peptides was assessed by fluorescence microscopy. Importantly, mice treated with fluorescein-conjugated

peptides displayed patchy areas of green fluorescence that was absent in vehicle-treated mice (Figure 5A). At this time point, no significant fluorescence could be detected in other organs, such as liver and kidneys (see Supplementary material online, Figure S2). Importantly, all treatments did not change cardiac mass (left ventricular weight/BW: vehicle = 3.5 ± 0.05 ; P_{cn} = 3.6 ± 0.05 ; P_{mit} = 3.7 ± 0.01 , not significant) or function (% fractional shortening after 3 days of treatment: vehicle = 51 ± 4.5 ; P_{cn} = 49 ± 3.7 ; P_{mit} = 52 ± 4.9 , not significant). However, FP_{mit} peptides markedly increased DHE staining of cardiac sections and *in vivo* mitochondrial ROS generation (Figure 5B). Furthermore, P_{mit} peptides markedly increased TUNEL staining of cardiac sections of treated mice (Figure 5C). Taken together, these results suggest that AKAP121 is an important regulator of mitochondrial function and cell survival *in vivo*, and thus

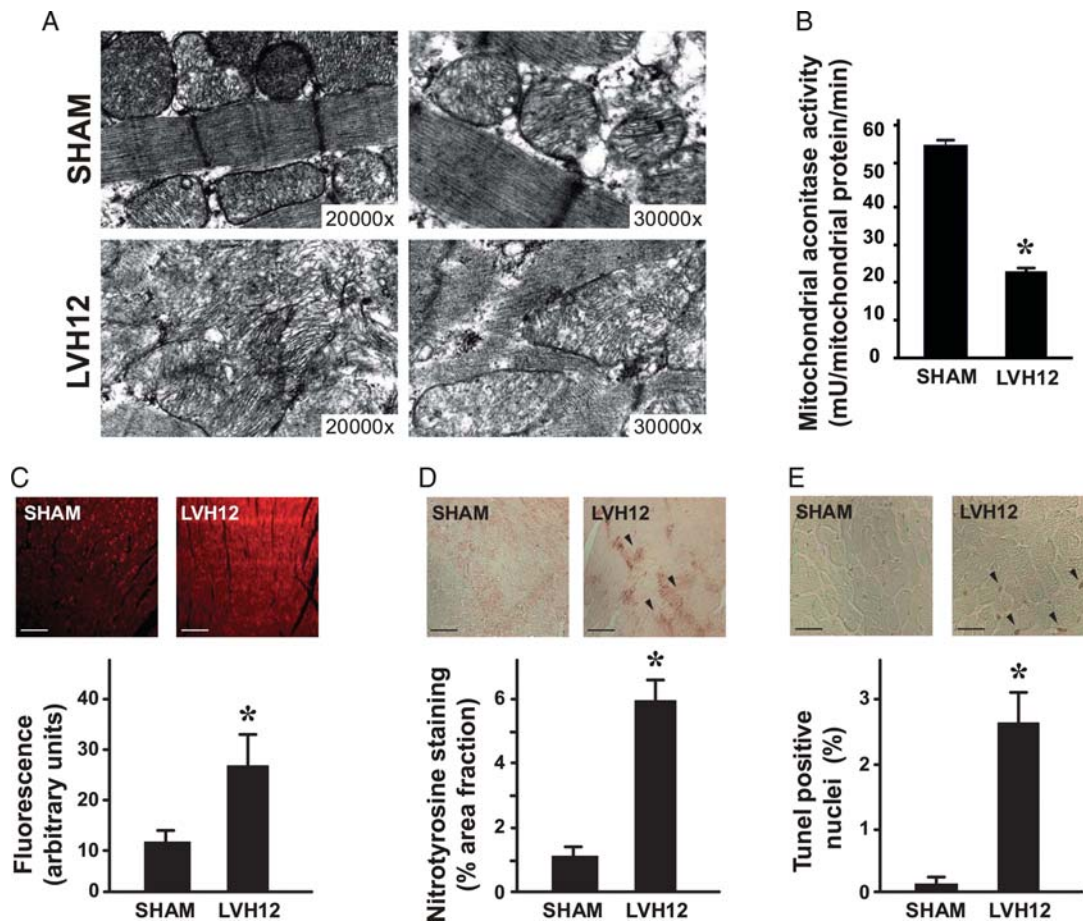


Figure 4 Mitochondrial function and ROS generation in the rat model of pressure overload. (A) Representative electron microscopy microphotographs of cardiac sections from SHAM and LVH12 rat hearts ($n = 4-6$ hearts/group; 20,000 \times and 30,000 \times magnification). (B) Mitochondrial aconitase activity in SHAM and LVH12 hearts ($n = 4$ hearts/group; $*P < 0.01$ vs. SHAM). (C) ROS production assessed by dihydroethidium (DHE) conversion to red fluorescent ethidium in SHAM and LVH12 hearts. (Top) Representative fluorescence staining of cardiac sections from SHAM and LVH12 rat hearts ($n = 3-4$ rats/group). Scale bar = 50 μm . (Bottom) Cumulative data of independent experiments ($*P < 0.0001$ vs. SHAM). (D, Top) Representative nitrotyrosine immunostaining in cardiac sections from rat SHAM and LVH hearts ($n = 3-4$ rats/group). Positive cells appear brown (arrow heads). Scale bar = 50 μm . (Bottom) Cumulative data of independent experiments ($*P < 0.01$ vs. SHAM). (E, Top) Representative TUNEL staining of cardiac sections from SHAM and LVH12 rat hearts counterstained with methyl green ($n = 4-5$ hearts/group). Positive nuclei appear brown (arrow heads). Scale bar = 50 μm . (Bottom) Cumulative data of independent experiments ($*P < 0.01$ vs. SHAM).

AKAP121 downregulation may represent an important event in the development of cardiac dysfunction.

4. Discussion

This study shows the effects of AKAP121 downregulation on mitochondrial function, ROS levels, and cell survival. *In vitro* and *in vivo* competitive displacement of AKAP121 from mitochondria induced mitochondrial dysfunction, increased ROS levels, and promoted cell death. Consistent with these results, downregulation of AKAP121 induced by pressure overload was associated with mitochondrial dysfunction, increased ROS production, and cell death. Taken together, these results suggest that AKAP121 is an important regulator of mitochondrial function and cell survival, and thus AKAP121 downregulation may represent an important event in the development of cardiac dysfunction.

Cardiac hypertrophy is characterized by marked abnormalities in cAMP signalling, initiated by the over-stimulation of β ARs, and activation of de-sensitization mechanisms.^{1,2} In response to pressure overload, downregulation of nuclear cAMP signals rapidly and significantly inhibited CREB phosphorylation, altering PKA-dependent transcription of CREB-induced genes, including AKAP121. Consistently, AKAP121 levels were also significantly reduced by chronic *in vivo* ISO administration (see Supplementary material online, Figure S3). Furthermore, AKAP121 is also subjected to ubiquitin-dependent degradation,²⁰ and this may be operating in the early phases of cardiac stress or after mitochondrial displacement by P_{mit} peptides, since we did not detect any increase in the cytosolic levels of AKAP121. Interestingly, ROS production itself also induced AKAP121 degradation *in vitro* (see Supplementary material online, Figure S4). The sources of ROS under conditions of pressure overload include the leakage from mitochondrial electron transport, xanthine oxidase, NADPH oxidase, NO synthase, and monoamine oxidase.²¹

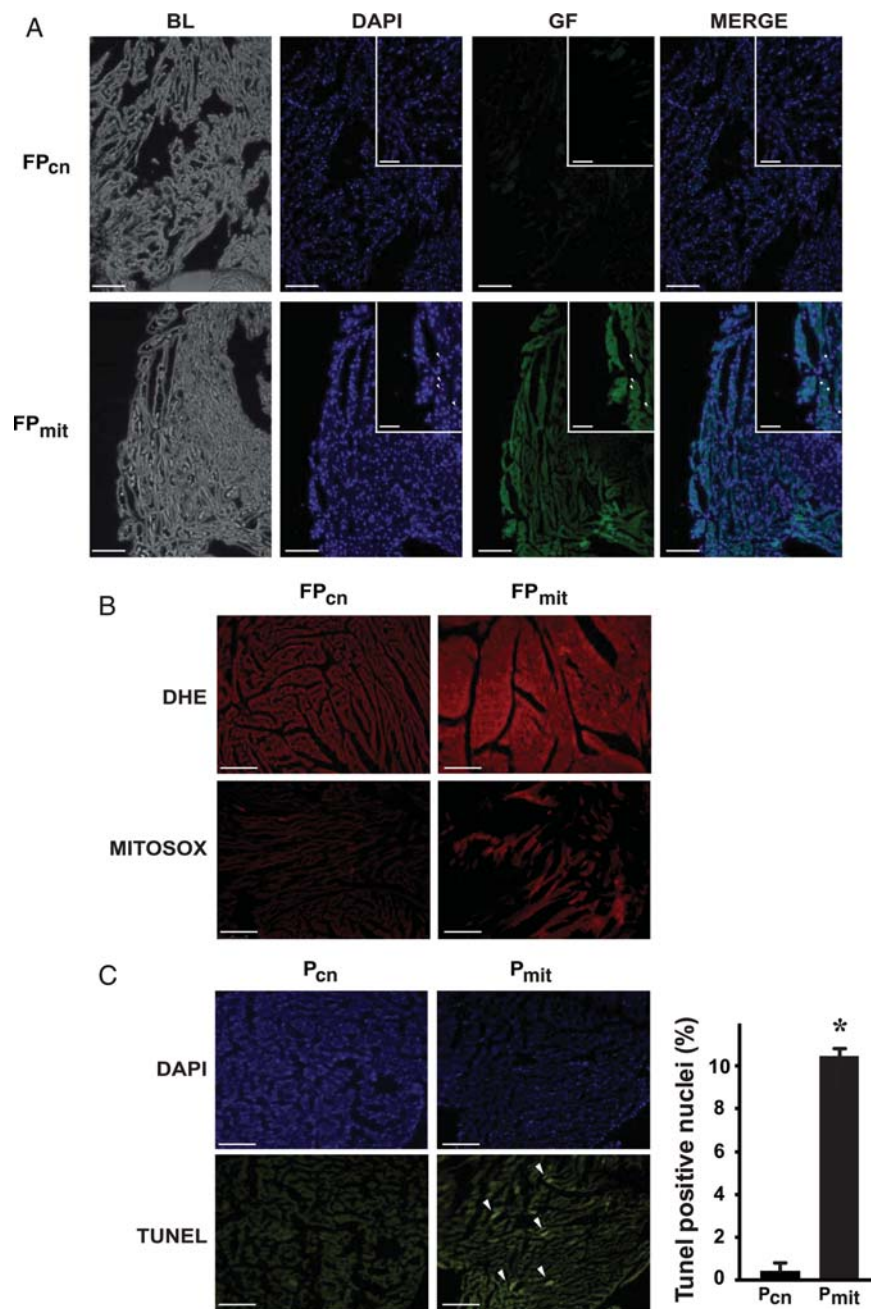


Figure 5 Effects of *in vivo* administration of AKAP121 delocalizing peptides. (A) Representative images of bright light (BL), DAPI staining, and green fluorescence (GF) of cardiac sections from wild-type mouse hearts treated with FP_{cn} or FP_{mit} peptides for 3 days ($n = 4$ hearts/group). Composites of DAPI and GF signals are shown on the right (MERGE). The white boxes in the upper right corner show magnified areas (arrow heads indicate nuclei, stars indicate perinuclear localization of FP_{mit} peptides). Scale bar = 250 μm in the larger images, or 30 μm in the magnified area. (B) Representative images of DHE staining (top) or Mitosox staining (bottom) of cardiac sections of wild-type mouse hearts treated with FP_{cn} or FP_{mit} peptides for 3 days ($n = 4$ hearts/group). Scale bar = 250 μm . (C, left panels) Representative DAPI (top) and TUNEL staining (bottom) in cardiac sections of mouse hearts treated with P_{cn} or P_{mit} peptides for 3 days. Positive nuclei appear green (arrow heads). (Right panel) Cumulative data of multiple independent experiments ($n = 4$ hearts/group; * $P < 0.01$ vs. SHAM). Scale bar = 250 μm .

All these mechanisms might contribute to ROS-mediated AKAP121 downregulation during pressure overload. Eventually, transcriptional silencing of the gene is responsible for the permanent loss of the protein from the mitochondria.

Recent studies have shown that AKAP121 negatively regulates cardiomyocytes hypertrophy *in vitro*, since the knockdown of AKAP121 expression releases an active pool of calcineurin, activates its

downstream effector NFAT (nuclear factor of activated T cells) and the hypertrophic gene program.¹⁵ While P_{mit} peptides induced *in vitro* NFAT nuclear translocation and expression of interleukin-6 (IL-6), a NFAT-regulated gene in SMCs (see Supplementary material online, Figure S5), the short-term *in vivo* administration of P_{mit} peptides did not induce cardiac hypertrophy. These results are consistent with our data demonstrating that hypertrophy development can be

dissociated *in vivo* from the activation of pathological molecular signaling pathways.¹ However, it is conceivable that prolonged treatment might indeed promote cardiac hypertrophy; alternatively, it is possible to speculate that 'delocalized' pools of AKAP121 *in vivo* might still bind and sequester calcineurin, thus preventing the activation of the hypertrophic gene program.

AKAP121 has a major role in targeting PKA close to several mitochondrial substrates, including the nuclear-encoded 18 kDa subunit of complex I (NDUFS4), enhancing the activity of mitochondrial respiratory complexes.²² Furthermore, PKA phosphorylates and inactivates the pro-apoptotic protein BAD, blocking its association with Bcl-2 and inhibiting apoptosis.²³ We have previously shown that AKAP121 also targets src to mitochondria, increasing mitochondria respiration, in part, through src.¹³ These, and other yet unidentified PKA/src substrates, might be involved in the development of mitochondrial dysfunction after AKAP121 uncoupling or downregulation.

Interestingly, while P_{mit} peptides promoted mitochondrial stress and increased oxidative stress in both SMCs and NVMs, the final outcome of the stress was different in these cells. In fact, SMC viability was unaffected by P_{mit} peptides under unstressed conditions, even if their tolerance to further stress was diminished. In contrast, P_{mit} peptides increased PI staining even in unstressed NVMs, suggesting that these cells are more vulnerable to AKAP121 downregulation, mitochondrial dysfunction and increased oxidative stress. Thus, cells retaining a higher replicating potential might be able to better tolerate oxidative stress under basal conditions.

Based on our results, we believe that resetting cAMP signal propagation to the nuclei and mitochondria despite pressure overload might represent a novel powerful strategy to preserve mitochondrial function and prevent excessive ROS generation. Thus, the identification of drugs or molecules that restore or stabilize AKAP-PKA or over-express AKAP121 in stressed cardiomyocytes, is expected to be beneficial and highly specific for the treatment of pressure overload-induced cardiac hypertrophy and heart failure.

In conclusion, our findings highlight a crucial role of AKAP121 in the maintenance of cellular homeostasis and mitochondrial activity. Downregulation of AKAP121 in response to pressure overload might constitute a previously unpredicted loop between dysregulation of cAMP signalling and mitochondria dysfunction. This might impact on oxidative stress and cardiomyocyte survival, leading to heart failure.

Supplementary material

Supplementary material is available at *Cardiovascular Research* online.

Acknowledgements

This paper is dedicated to the memory of M.C. passed away on March 23rd 2010.

Conflict of interest: none declared.

Funding

This work was partly supported by Associazione Ricerca contro il Cancro (IG 2008-2009 to V.E.A. and A.F.), and by Fondo Internazionale per la

Ricerca di Base (FIRB) grants (FIRB 2007 to V.E.A.) and by Programmi di Ricerca di Interesse Nazionale (PRIN) grants from Ministero dell'Università e della Ricerca Scientifica (MIUR) (200884K784_003, 2007-08 to V.E.A., 2007KS47FW_002 to A.F., 2006062917_002 to G.E., 2007WS3JL3 to M.C.).

References

- Perrino C, Naga Prasad SV, Mao L, Noma T, Yan Z, Kim HS et al. Intermittent pressure overload triggers hypertrophy-independent cardiac dysfunction and vascular rarefaction. *J Clin Invest* 2006;**116**:1547–1560.
- Rockman HA, Koch WJ, Lefkowitz RJ. Seven-transmembrane-spanning receptors and heart function. *Nature* 2002;**415**:206–212.
- Zakhary DR, Moravec CS, Bond M. Regulation of PKA binding to AKAPs in the heart: alterations in human heart failure. *Circulation* 2000;**101**:1459–1464.
- Mauban JR, O'Donnell M, Warriar S, Manni S, Bond M. AKAP-scaffolding proteins and regulation of cardiac physiology. *Physiology (Bethesda)* 2009;**24**:78–87.
- Dodge-Kafka KL, Langeberg L, Scott JD. Compartmentation of cyclic nucleotide signaling in the heart: the role of A-kinase anchoring proteins. *Circ Res* 2006;**98**:993–1001.
- Indolfi C, Stabile E, Coppola C, Gallo A, Perrino C, Allevato G et al. Membrane-bound protein kinase A inhibits smooth muscle cell proliferation *in vitro* and *in vivo* by amplifying cAMP-protein kinase A signals. *Circ Res* 2001;**88**:319–324.
- Carnegie GK, Soughayer J, Smith FD, Pedroja BS, Zhang F, Diviani D et al. AKAP-Lbc mobilizes a cardiac hypertrophy signaling pathway. *Mol Cell* 2008;**32**:169–179.
- Pare GC, Bauman AL, McHenry M, Michel JJ, Dodge-Kafka KL, Kamiloff MS. The mAKAP complex participates in the induction of cardiac myocyte hypertrophy by adrenergic receptor signaling. *J Cell Sci* 2005;**118**:5637–5646.
- De Windt LJ, Lim HW, Bueno OF, Liang Q, Delling U, Braz JC et al. Targeted inhibition of calcineurin attenuates cardiac hypertrophy *in vivo*. *Proc Natl Acad Sci USA* 2001;**98**:3322–3327.
- Carlucci A, Lignitto L, Feliciello A. Control of mitochondria dynamics and oxidative metabolism by cAMP, AKAPs and the proteasome. *Trends Cell Biol* 2008;**18**:604–613.
- Feliciello A, Rubin CS, Avvedimento EV, Gottesman ME. Expression of a kinase anchor protein 121 is regulated by hormones in thyroid and testicular germ cells. *J Biol Chem* 1998;**273**:23361–23366.
- Cardone L, Carlucci A, Affaitati A, Livigni A, DeCristofaro T, Garbi C et al. Mitochondrial AKAP121 binds and targets protein tyrosine phosphatase D1, a novel positive regulator of src signaling. *Mol Cell Biol* 2004;**24**:4613–4626.
- Livigni A, Scorziello A, Agnese S, Adornetto A, Carlucci A, Garbi C et al. Mitochondrial AKAP121 links cAMP and src signaling to oxidative metabolism. *Mol Biol Cell* 2006;**17**:263–271.
- Scholten A, van Veen TA, Vos MA, Heck AJ. Diversity of cAMP-dependent protein kinase isoforms and their anchoring proteins in mouse ventricular tissue. *J Proteome Res* 2007;**6**:1705–1717.
- Abrenica B, AlShaaban M, Czubryt MP. The A-kinase anchor protein AKAP121 is a negative regulator of cardiomyocyte hypertrophy. *J Mol Cell Cardiol* 2009;**46**:674–681.
- Indolfi C, Di Lorenzo E, Perrino C, Stingone AM, Curcio A, Torella D et al. Hydroxymethylglutaryl coenzyme A reductase inhibitor simvastatin prevents cardiac hypertrophy induced by pressure overload and inhibits p21ras activation. *Circulation* 2002;**106**:2118–2124.
- Feliciello A, Gottesman ME, Avvedimento EV. cAMP-PKA signaling to the mitochondria: protein scaffolds, mRNA and phosphatases. *Cell Signal* 2005;**17**:279–287.
- De Capua A, Del Gatto A, Zaccaro L, Saviano G, Carlucci A, Livigni A et al. A synthetic peptide reproducing the mitochondrial targeting motif of AKAP121: a conformational study. *Biopolymers* 2004;**76**:459–466.
- Baschong W, Suetterlin R, Laeng RH. Control of autofluorescence of archival formaldehyde-fixed, paraffin-embedded tissue in confocal laser scanning microscopy (CLSM). *J Histochem Cytochem* 2001;**49**:1565–1572.
- Carlucci A, Adornetto A, Scorziello A, Viggiano D, Foca M, Cuomo O et al. Proteolysis of AKAP121 regulates mitochondrial activity during cellular hypoxia and brain ischaemia. *EMBO J* 2008;**27**:1073–1084.
- Takimoto E, Kass DA. Role of oxidative stress in cardiac hypertrophy and remodeling. *Hypertension* 2007;**49**:241–248.
- Papa S, Scacco S, Sardanelli AM, Petruzzella V, Vergari R, Signorile A et al. Complex I and the cAMP cascade in human physiopathology. *Biosci Rep* 2002;**22**:3–16.
- Harada H, Becknell B, Wilm M, Mann M, Huang LJ, Taylor SS et al. Phosphorylation and inactivation of BAD by mitochondria-anchored protein kinase A. *Mol Cell* 1999;**3**:413–422.